Comparative analysis between Singular Spectral Analysis and Empirical Mode Decomposition for Structural Damage Detection

Elisa C. González, Gladys E. Salcedo, Leonardo Cano

Abstract

Context: Due to technological advances in instrumentation and digital signal processing, non-invasive methods for detecting structural damage have become increasingly important in recent years. Vibration-based structural health monitoring techniques (SHM) allow the identification of presence and location of damage from permanent changes in the fundamental frequencies of the signals. A method successfully employed focused on damage detection is the Empirical Mode Decomposition (EMD). Another underutilized method in this field of study is the Singular Spectral Analysis (SSA). In this paper, we describe both methodologies and perform a simulation study to compare them and identify which one is more effective in detecting structural damage.

Method: We applied the methods on a reference study known as benchmark SHM problem to facilitate the comparison between the methods. In order to evaluate the effectiveness of both methods, we proposed to perform a Monte Carlo type simulation study. To control the included random noise and other factors inherent to the simulation, we repeated the procedure 1000 times for each type of damage.

Results: When the damage is severe, both methods have good performance. However, when the damage is slight, the change in fundamental frequency is not apparent. But we observed a significant change in the amplitude level, in this case the SSA perform the best results.

Conclusions: The EMD and SSA methods, along with a high pass filter, detects severe damage when the acceleration records have low or no noise. When the acceleration records are contaminated with noise, the likelihood of the EMD detecting the damage decreases dramatically. One of the advantages of the SSA over the EMD is that, for medium or mild damage patterns, the SSA does not require filters or the use of the Hilbert transform to detect the damage. In general, we found that SSA is more effective in detecting damage.

Keywords: Hilbert-Huang Transform, Signal Analysis, Structural Health Monitoring, Time-Frequency Analysis.

Resumen

Contexto: Debido a los avances tecnológicos en instrumentación y procesamiento digital de señales, los métodos no invasivos para la detección de daños estructurales han ganado cada vez mayor importancia en los últimos años. Las técnicas de monitoreo de salud estructural basadas en vibraciones (SHM) permiten identificar la presencia y ubicación del daño a partir de cambios permanentes en las frecuencias fundamentales de las señales. Un método que se ha implementado con éxito enfocado a la detección de daño es la descomposición modal empírica (EMD) y otro método poco explorado en este campo de estudio, es el análisis singular espectral (SSA). En este artículo describimos ambas metodologías y realizamos un estudio de simulación para compararlas e identificar cuál de ellas es más efectiva en la detección del daño estructural.

Método: Aplicamos los métodos en un estudio de referencia conocido como SHM para facilitar la comparación entre los métodos. Para evaluar la efectividad de ambos métodos se propone un estudio de simulación tipo Monte Carlo. Para contralar la inclusión de ruido aleatorio y otros factores inherentes a la simulación el procedimiento fue repetido 1000 veces para cada tipo de daño.
Resultados: Cuando el daño es severo ambos métodos tienen buen desempeño. Cuando el daño es leve el cambio en la frecuencia fundamental no es aparente, pero se observo un cambio significativo en el nivel de amplitud, en este caso el método SSA se conduce a mejores resultados.
Conclusiones: Los métodos EMD y SSA junto con filtros pasa altos cuando los registros de aceleración no tienen ruido o este es bajo. Cuando los registros de aceleración están contaminados con ruido la probabilidad de detección de daño del EMD decrece drásticamente. Una de las ventajas del SSA sobre el EMD es que para patrones de daño medios, este no requiere filtros o el uso de la transformada Hilbert para detectar el daño. En general se encontró que el SSA es más efectivo para la detección del daño.
Palabras clave: Transformada Hilbert-Huang, Análisis de Señales, Monitoreo de Salud Estructural, Análisis Tiempo-Frecuencia.

1. Introduction

1.1. General Aspects

In recent decades, some researchers paid special attention to avoid sudden failure of structural components through early detection of damage. Therefore, there are several techniques for damage analysis including vibrations-based methods. However, it is necessary to implement a time series-based algorithm for the monitoring to process the large amount of information provided by sensors and simplify it to measure the structural condition.

Some methodologies that give good results for damage detection are the Hilbert-Huang Transform (HHT), which combines EMD with Hilbert Spectral Analysis. Additionally, a new approach is the SSA, which has been employed in recent years; in [1] and [2] claim that singularities can be associated with cracks, damage, or environmental changes. Specifically, SSA is a time-series analysis technique that decomposes the signal into specific principal components that describe its trend, fundamental frequencies, and singularity effects.

EMD and SSA allows decomposing a signal into monocomponent signals (signals with a single fundamental frequency). Once the decomposition is obtained, it is possible to use Hilbert Spectral Analysis to study the decomposed signals in the time-frequency domain and observe whether there is a change in the natural frequencies, i.e., structural damage and this is valid in a wide field of applications, for example for the detection of brain damage [3].
.
This study compares the effectiveness of these two methods for detecting structural damage based on a simulation study applying these methodologies to the dynamic acceleration response of a four-story steel structure that contains different damage patterns. We generated this acceleration response through a computer program called Datagen, which simulates a reference problem known as the benchmark SHM problem developed by the structural health research group IASC-ASCE [4].

1.2. Background

Structural health monitoring based on the vibration of structures is one of the main reasons why different tools are developed to study structural damage from changes in natural frequency, since this is associated with the mass and stiffness matrix of the structure. Generally, the mass tends to remain constant, so if there are changes in frequency, these will be caused by changes in stiffness; if this variation is preserved over time, then there is damage in the structure, for example, in [5] performed a modal identification and detection of damage in beam-type structures by studying methods based on natural frequency changes.

In [6] uses instantaneous phase data obtained from a single-component decomposition for damage detection of a three-story building. In [7] proposed a damage index called the "EMD energy damage index" for structural damage detection, and corroborated its applicability through numerical and experimental studies. In [8] presents the state of the art on the beginnings and advances in diagnostic and damage detection studies, and develops a new methodology for system identification and damage detection using actual output data from vibration records, based on the direct application of Time and Frequency Averaging Representation (MTFR) and Frequency Domain Decomposition (FDD).

In [9] performs a comparative review study on different damage detection methods, including ARMA models, parameter identification tools, NexT/ERA identification systems, damage index, EMD, EMD+ HHT (Hilbert-Huang Transform), AR models, and others. These methods applied to the benchmark problem allow analyzing the advantages and disadvantages of each of these methods and their detection capability for different damage patterns.

Recent research implements different methodologies for vibration-based damage detection. For example, in [10] uses the recursive spectral singular analysis algorithm to identify structural damage, using inputs a single channel in real time and produces a lagged Hankel time matrix of the series; This method allows obtaining information about the current state of the structure, in this case a cantilever beam subject to seismic excitation. [11] proposes the multivariate empirical modal decomposition for the location of damage in structures using measurements. [12] uses the EMD with adaptive noise to identify the presence, location, and severity of damage in a steel truss bridge model; In this paper, they build the object of study under laboratory conditions and they experimentally subject the bridge to white noise excitations.

In [9] confirms that EMD, together with Hilbert transform, can detect specific damage patterns. Then, this paper verifies this result and also implements the SSA, which is still an innovative algorithm for structural damage detection in the field of civil engineering.

2. Materials and methods

In this section, some concepts regarding damage are briefly explained as well as some mathematical concepts that are associated with the time-frequency analysis methods.

2.1 Levels of Structural Damage

In civil engineering, the concept of damage has different meanings and interpretations. In this study, structural damage is defined as changes (almost always permanent) of structural properties such as stiffness, strength, dynamic properties, or losses of acceptable structural performance according to pre-established behavioral criteria [8].

The effects of damage in a structure can be classified into four levels as follows [13]:

- Level 1. Determines the presence of damage in the structure.
- Level 2. Level 1+ determines the geometric location of the damage.
- Level 3. Level 2+ the quantification of the severity of the damage.
- Level 4. Level 3+ the prediction of the remaining service-life of the structure.

Generally, vibration-based damage identification methods that do not use a structural model mainly provide Level 1 and 2 damage identification.

2.2 Empirical Mode Decomposition (EMD)

EMD is a methodology for decomposing a given signal into a set of elementary signals called "Intrinsic Mode Functions" (IMFs), defined by the following conditions [14]:

1) The number of extremes (max and min) and zero crossings must not differ by more than one.
2) At any instant, the average between the envelope of maximum points and envelope of minimum points must be close to zero.

The iterative procedure proposed by Huang to obtain the IMFs is as follows:

1) Identify the extreme points of the function $x(t)$ (max and min)
2) Interpolate between the maximum points using a cubic spline to obtain an envelope $e_{\max}(t)$ similarly with the minimum points to obtain $e_{\min}(t)$. The envelopes should cover the entire signal.
3) Calculate the average of the envelopes $m(t) = \frac{(e_{max}(t) + e_{min}(t))}{2}$
4) Calculate $h(t) = x(t) - m(t)$, where $h(t)$ is the IMF candidate. Steps 1) through 4) should be iterated with $h(t)$ as the new function until the two conditions described above for IMFs are met.
5) Once the conditions have been met, $h(t)$ becomes the first IMF.
6) Calculating the residue $r(t) = x(t) - \sum IMF$, $r(t)$ becomes the new function, and the steps are repeated to find the next $\sum IMF$.
7) The procedure is repeated until the residual can be considered negligible or constitutes a monotonic function (no max or min).

In summary, this process is based on generating envelopes defined by max and min of a series and subtracting the average of these envelopes from the initial series.

2.3 Singular Spectral Analysis (SSA)

This method incorporates classical time series analysis elements, like classical spectral analysis [15], digital signal processing, dynamic systems, and multivariate statistics. SSA consists of the decomposition of an original signal into a set of uncorrelated components from which three characteristics can be extracted: trend, oscillation, and noise [16] [17]. Such decomposition is based on the Karhunen-Löeve covariance matrix. This procedure is developed in four steps:

1) Step 1: Decomposition of the time series

Let $Y=\{y_1,y_2,\ldots,y_N\}$ be the observed series time of size N . Consider the matrix X of dimension $L\times K$ given by

$$X=\begin{bmatrix} X_1 \\ \vdots \\ X_K \end{bmatrix}^T=\begin{bmatrix} y_1 & y_2 & y_3 & \cdots & y_K \\ y_2 & y_3 & y_4 & \cdots & y_{K+1} \\ y_3 & y_4 & y_5 & \cdots & y_{K+2} \\ \vdots & \vdots & \vdots & \ddots & \vdots \\ y_L & y_{L+1} & y_{L+2} & \cdots & y_N \end{bmatrix}, \quad (1)$$

L is the length of the window such that $2\le L\le N, K=N-L+1$ is the number of column of the matrix X and each $X_i=\left(y_i,\ldots,y_{i+L-1}\right)^T, 1\le i\le K.$ Choosing the length L is one of the biggest challenges when working with SSA, mainly for non-stationary series, since a large window may require higher computational efforts, and a small window may separate the noise from the trend components.

Note that X is a matrix of trajectories known as the Hankel matrix, with the property that the component $y_{i,j}$ of row i and column j satisfies that $y_{i,j}=y_{i-1,j+1}=y_{i+1,j-1}$, leading to X have equal elements over the antidiagonals.

2) Step 2: Decomposition of X into singular values (SVD)

Let $W=XX^T$ be a square matrix $L\times L$, then we find the positive eigenvalues $\left(\lambda_1>\lambda_2>\ldots>\lambda_d\right)$ of W and their corresponding eigenvectors $U_1,U_2,\ldots,U_d$. The square root of the eigenvalues $\sqrt{\lambda_i}$ of W are known as the singular values of the matrix X and

the corresponding eigenvectors U_i are the left singular vectors of the matrix X .

Other singular vectors computed by Equation (2) refer to the right singular vectors of the matrix X,

$$V_i = \frac{X^T U_i}{\sqrt{\lambda_i}}, \qquad i = 1, \ldots, d \tag{2}$$

Each eigentriplet $\left(\sqrt{\lambda_i}, U_i, V_i\right)$ of the matrix X determines the corresponding components and all eigentriplets determine a d -dimensional subspace in R^L . Then,

$$X_i = \sqrt{\lambda_i} U_i V_i^T, \tag{3}$$

and the matrix X can be expressed as

$$\tilde{X} = \tilde{X}_1 + \tilde{X}_2 + \ldots + \tilde{X}_d. \tag{4}$$

3) Step 3: Grouping of eigentriplets

This step selects the desired components among all the components that were obtained in Step 2; usually, the selection criterion is made a priori, which can be a problem since the SSA projects the original data into different orthogonal components, but it is not easy to find all the components with the required information since this depends on the window length that was chosen in Step 1.

Once we obtain the expression (2), in this step, the set of indexes is partitioned $1, \ldots, d$ in m disjoint subsets $I_1, \ldots, I_m$. Let $I = i_1, \ldots, i_p$ then the resulting matrix X_I corresponding to group I is defined as $X_I = X_{i_1} + \ldots + X_{i_p}$, these matrices are calculated for each group $I_1, \ldots, I_m$ and the expansion of (2) leads to the decomposition

$$X = \tilde{X}_{I_1} + \tilde{X}_{I_2} + \ldots + \tilde{X}_{I_m}. \tag{5}$$

The procedure of choosing the sets $I_1, \ldots, I_m$ is called eigentriplet clustering; furthermore, a relation given by (6) can be defined, which quantifies the degree of approximation the windows of the original signal.

$$R = \frac{\sum_{i \in I} \lambda_i}{\sum_{i=1}^{d} \lambda_i}. \tag{6}$$

4) Step 4: Averaging of the diagonals.

In the reconstruction of the required signal from the selected components, each matrix X_{I_j} of the decomposition given in Equation (5) is transformed into a new series of length N, using the procedure of averaging over the diagonals, which defines the value of the time series as an average of the diagonals corresponding to each matrix in X_{I_j}.

This procedure is based on the following: let $Q=(q_{i,j})$ be any $L\times K$-size matrix, each element $q_{i,j},(i+j=l)$ becomes an element of Hankel's matrix, thus

$$\tilde{q}_{i,j}=\begin{cases}\dfrac{1}{l-1}\displaystyle\sum_{m=1}^{l-1}q_{m,l-m}, & 2\le l\le L-1.\\[2ex] \dfrac{1}{L}\displaystyle\sum_{m=1}^{L}q_{m,l-m}, & L\le l\le K+1.\\[2ex] \dfrac{1}{K+L-l+1}\displaystyle\sum_{m=1-K}^{L}q_{m,l-m}, & K+2\le l\le K+L.\end{cases} \tag{7}$$

This is known as the Hankelization procedure and applying it to all components of X_{I_j} matrices produce a reconstructed series $\tilde{X}^{(k)}=\left(\tilde{x}_1^{(k)},\ldots,\tilde{x}_N^{(k)}\right)$. Therefore, the initial series $y_1,y_2,\ldots,y_N$ is decomposed into the sum of m reconstructed series, as follows:

$$\tilde{Y}_t=\sum_{k=1}^{m}\tilde{x}_t^{(k)}, \qquad t=1,\ldots,N. \tag{8}$$

Each component contributes part of the retained energy obtained from the original series; clearly, the greater the number of components, the greater the information collected from the initial series. For this reason, another challenges in working with SSA: identifying the number of components to be used in the reconstruction procedure. In order to solve this, specific experimental tests are performed together with the eigenvalue analysis in order to have better accuracy in choosing the number of components needed for the reconstruction process.

The residual r_t can be calculated by considering the difference between both series, the original and the reconstructed series, as follows:

$$r_t=Y_t-\tilde{Y}_t. \tag{9}$$

2.4 Structural Health Monitoring Benchmark Problem

Applying different methodologies to different structures can generate specific difficulties when making comparisons between them. In this sense, the structural health monitoring research group IASC-ASCE developed a series of reference problems known as benchmark SHM problems divided into two phases. This section details the first phase of this study, based on the simulated response of a test structure, on which the two methodologies for damage detection will be applied.

2.4.1 Benchmark Structure

The benchmark problem structure is a four-story steel structure with three portal frames in each direction, 2.50 m spans, and 3.60 m floor height. The elements are made of 300 W hot rolled steel with a nominal yield strength of 300 MPa. The sections are unusually designed for a scale model. All columns are oriented so that their strong axis is in the x-direction and their weak axis in the y-direction. To the inter-story beams, their strong axis is in the z-direction. There are two diagonal suspenders on each floor of each exterior face, which can be removed to simulate damage. There is one floor slab per compartment; four 800 kg slabs on the first level, four 600 kg slabs each on the second and third levels, and the fourth level there are four 400 kg slabs or three 400 kg slabs and one 550 kg slab to create some mass asymmetry.

Through the benchmark problems and using the finite element method, it is possible to generate a dynamic analysis in time with 12 or 120 degrees of freedom (DOF). The 12 DOF restricts all motions except two horizontal translations and one rotation per floor, and the 120 DOF has only one constraint. The nodes at the base have the exact horizontal translation and rotation in the plane. On the other hand, the columns and floor beams are modeled as Euler-Bernoulli beams, and the braces are bars without bending stiffness [4].

The damage patterns introduced in the structure are shown in Table 1 and the damage patterns are shown in Figure 1. In reference [9] affirms “removal of braces in the story, which leads to stiffness reduction, is considered as major damage scenario and the weakening of beam column joint by loosening of bolts or reduction of stiffness for braces is considered as minor damage scenario of the structure.” Therefore, the severe damage patterns include patterns 1 and 2, the medium damage patterns are patterns 3, 4, and 5, and the slight damage pattern is pattern 6. The modeled damage patterns are predefined, and the analysis is carried out accordingly.

Table I
Benchmark Problem Damage Cases [9]

Damage patterns	*Damage Nature*
Damage patterns 1	No stiffness in 1st floor braces
Damage patterns 2	Damage pattern 1+ No stiffness in 3rd floor braces
Damage patterns 3	No stiffness is one 1st floor brace
Damage patterns 4	Damage pattern 3 + No stiffness in one 3rd floor brace
Damage patterns 5	Damage pattern 4+ beam-column connection weakened
Damage patterns 6	2/3 stiffness in one 1st floor brace

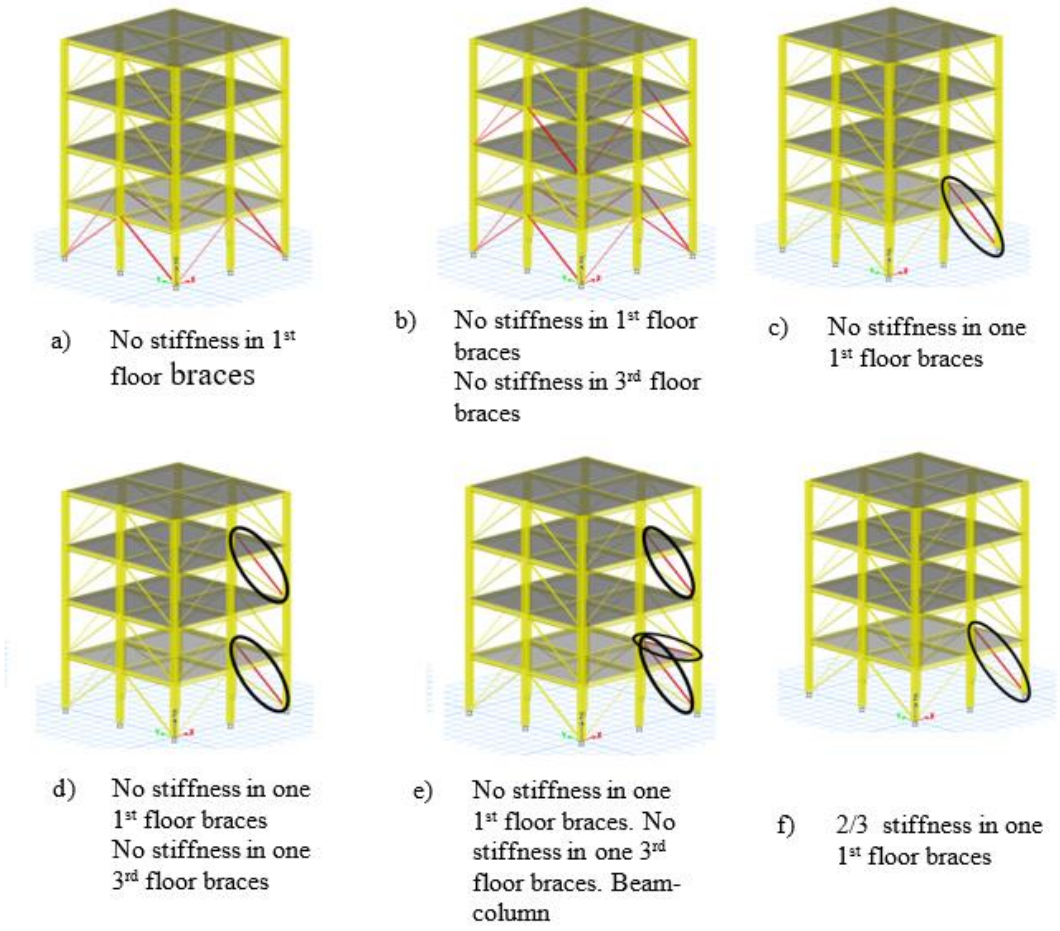

Figure 1. The damage scenarios for benchmark structure [9]

4. Results

4.1 Identification of Damage Time Instants and Locations

To study the sensitivity of these methods in detecting these damages, Table II sets some parameters in the simulation study of the benchmark problem; the force is calculated using the FAST Nigam-Jennings method, 1% damping is fixed to the critical. Similarly, all

acceleration records were simulated up to 80s; for clarity of the graphics, only 30s and 50s are shown in the figures, both for the EMD and the SSA.

Table II
Fixed Model Parameters in the Simulation Study

Parameter	***Value***
e	1%
dt	0.001
t	80 s
F	150
Findx	1

Figure. 2 we can observe the acceleration records of the first and second floors for damage pattern 1 and 2, respectively, without noise. To these signals, we applied a high pass filter=250 Hz. In Figures 3(a), 3(b), we observed that on the first floor, the damage occurs at 35s, while, in the second floor, the damage occurs at 40s. It is clear from the results that, if the noise pollution is either zero or very small, the EMD method is capable of detecting the damaging time instants and locations. The same happens when applying the SSA, in its Reconstructed Components (RCs) in Figure 4, in the first floor, the peak occurs at 35s and in the second floor at 40s.

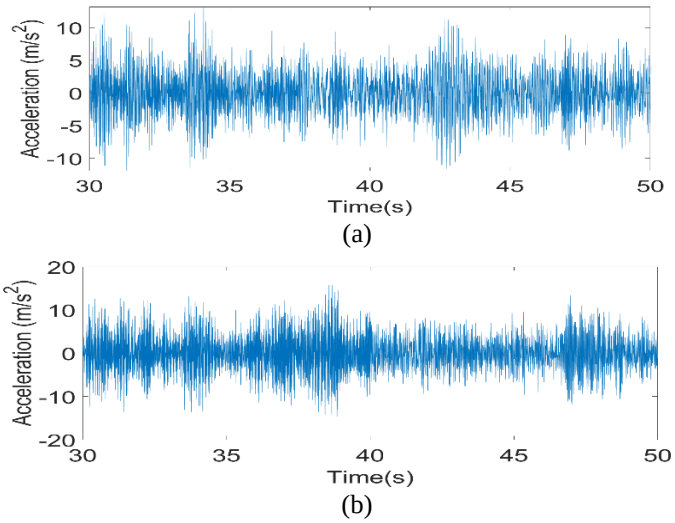

Figure 1 Acceleration records: (a) first floor, (b) second floor. All graphs correspond to damage pattern 2.

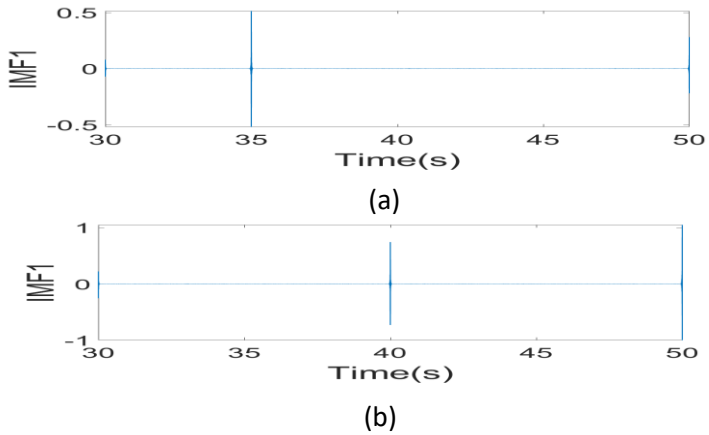

Figure 3 IMF1: (a) First Floor, (b) Second Floor. All graphs correspond to damage pattern 2.

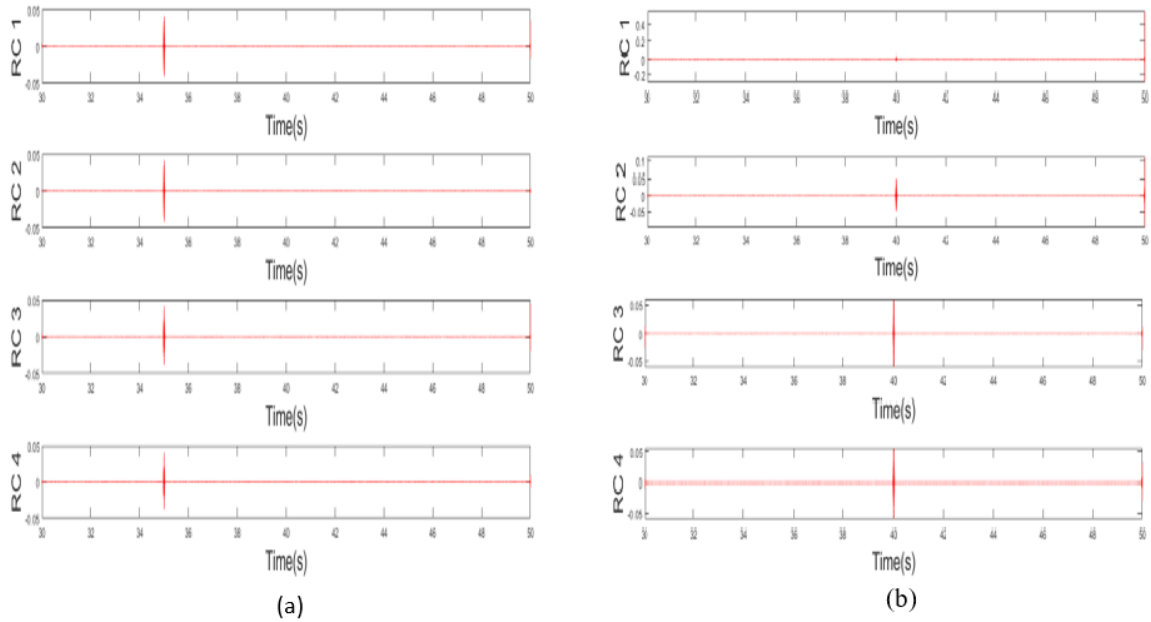

Figure 4 RC for damage pattern 1 and 2: (a) first floor, (b) second floor

When the acceleration records are polluted by noise and if the resulting magnitude of the damage spike is smaller than the noise levels, then the damage spike will merge in the noise. For example, in Figure 5, we generated a signal with a noise level of 10% and damage pattern 2. It corresponds to the acceleration records of the first floor.

It is worth mentioning that the model considers two sensors on each floor (one on the left side and the other on the right side); therefore, there are two acceleration records for each floor. Figure 2 only shows one acceleration record per floor since both are identical when the structure is symmetrical and the signal is not contaminated. However, when the signal contaminates with noise, acceleration records of each sensor per floor are different. But in this paper, we only show the sensor on the right side of the first floor as shown in Figure 5.

By processing the signals through the EMD, we obtained the first IMF presented in Figure 6 using a high pass=250 Hz to filter the sensor signal on the right side. However, it was not possible to identify the discontinuity peak which is confused with noise in either of them. According to [18], the ability of the EMD to detect signal damage at a noise level of 10% is about 30% in the benchmark problem.

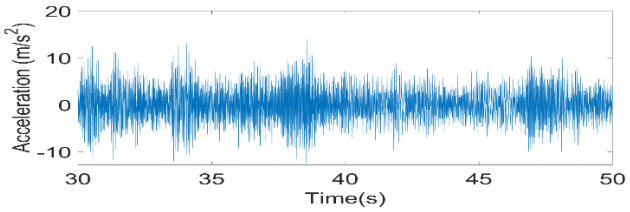

Figure 2. First floor acceleration records for damage pattern 2: Sensor on the right side

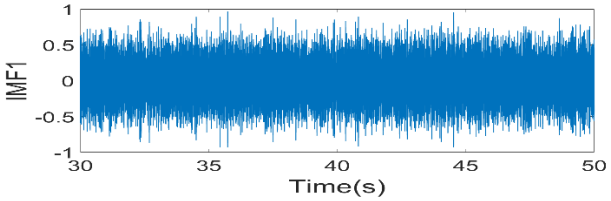

Figure 3. First IMFs for damage pattern 2 with a highpass filter: Sensor on the right side of the first floor

To overcome this difficulty, first we identified if there is a change in frequencies (i.e., if there is damage) using the Fourier transform and then we used the Hilbert-Huang transform to identify the instant at which this change occurs. In Figure 7, we applied the Fourier transform to acceleration records, where we observed that each of the four natural frequencies is divided into two frequencies. This division may indicate the occurrence of damage and it is quite evident in the first and second natural frequency.

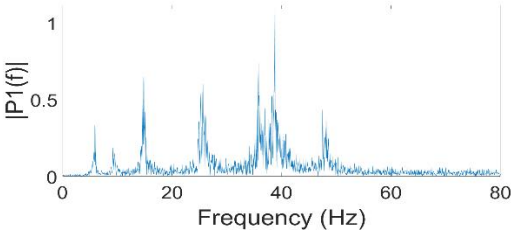

Figure 4. Fourier transform for damage pattern 2: Sensor on the right side of the first floor

To identify the instant in which the damage occurs, we decided to use a bandpass filter and to perform the frequency-time decomposition using the Hilbert-Huang transform. Figure 7 show that the first natural frequency could be between 5 Hz and 10.5 Hz. Therefore, we used a bandpass filter (bandpass (X,[5 10.5], Fs)), then we applied the EMD as shown in Figure 8; the first plot corresponds to the filtered signal and the others are the IMFs corresponding to the decomposition of the measured signal in the first modal response. Applying the Hilbert-Huang transform to all the IMFs, we obtained the frequency-time decomposition of the first modal response.

Figure 9 shows the frequency vs. time. We observed that the average frequency of the first mode changes from 9.6 Hz to 5.6 Hz at time instant t=40s. Therefore, we detected the time instant in which the damage occurs accurately. Although in the other modal responses, the splitting of the natural frequencies is not so prominent. If we apply the Hilbert-Huang transform, the frequency vs. time plots also show that the change occurs at the 40s.

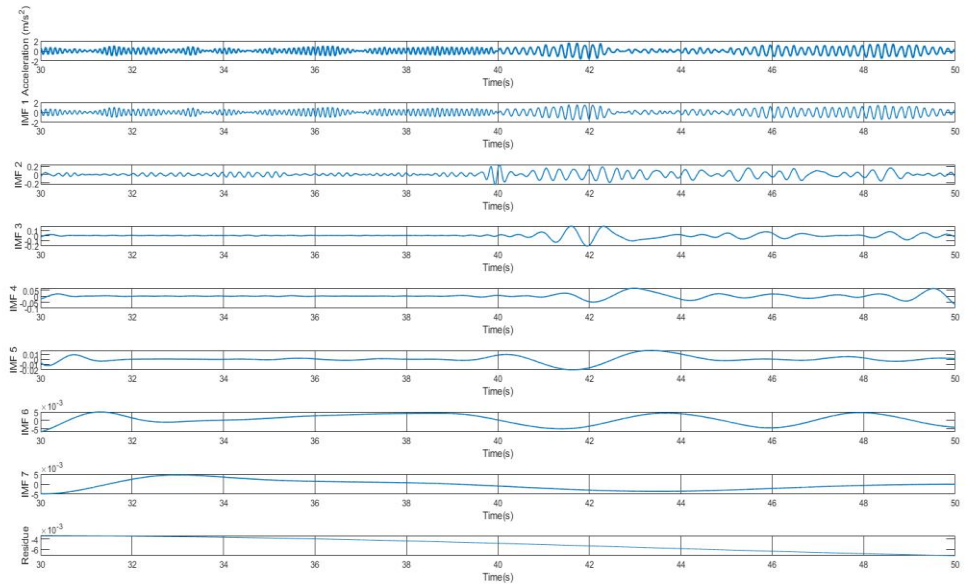

Figure 5. EMD for damage pattern 2 with a bandpass filter: Sensor on the right side of the first floor

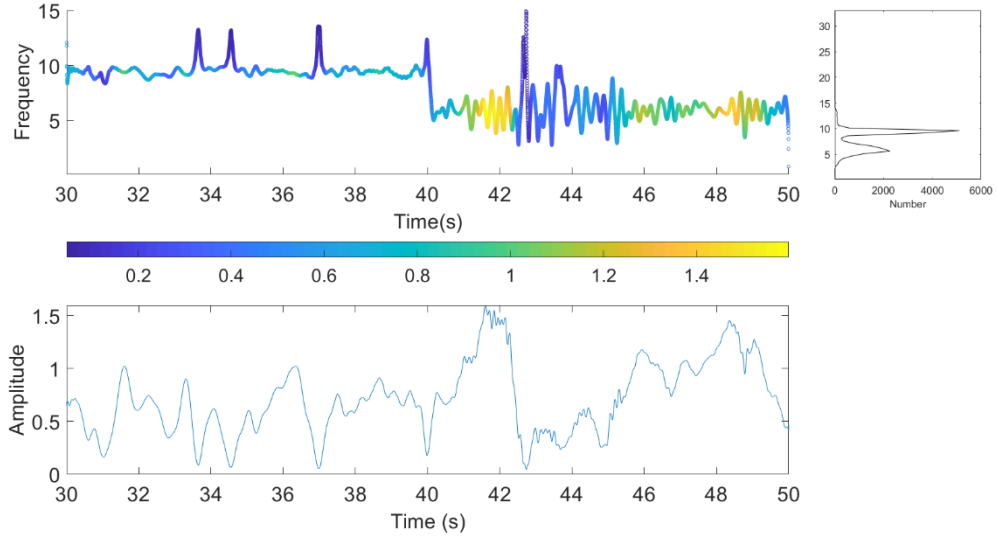

Figure 6. Hilbert-Huang transform for the first modal response (damage pattern 2): Sensor on the right side of the first floor.

Then we applied the SSA. In Figure 10, we presented the reconstructed components (RC) of this method; we applied to the signal a bandpass filter (bandpass (X,[5 10.5], Fs)). Although in the RC1 and RC2 components, we already observed a change in the signal behavior at 40s, we decided to apply the Hilbert transform to each of these RCs. In Figure 11, we present the Hilbert transforms of RC1 for the sensor. We observed that the average frequency of the first mode changes from 9.6 Hz to 5.6 Hz at t=40s. Therefore, we detected accurately when the damage occured using the SSA, and the results agree with the EMD's results.

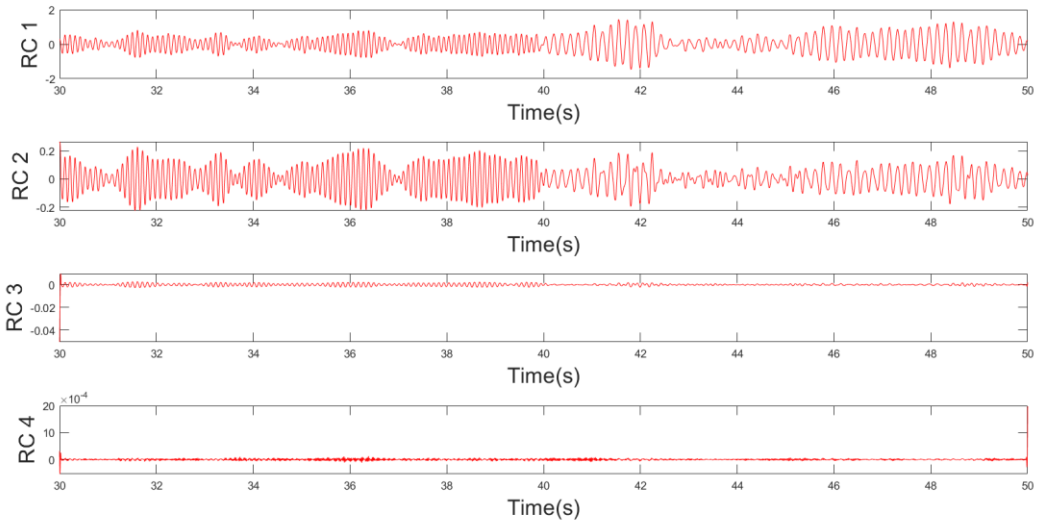

Figure 7 RC for damage pattern 2: Sensor on the right side of the first floor.

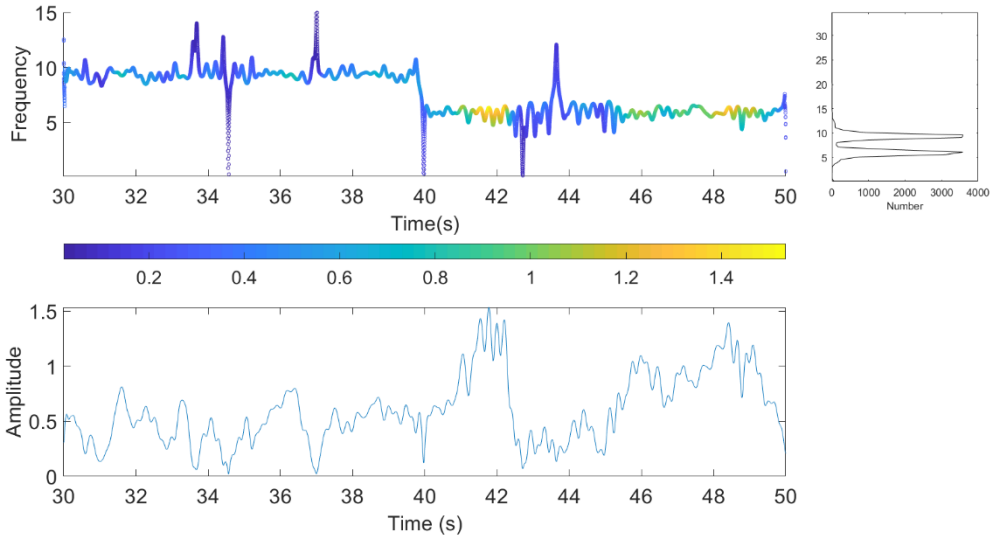

Figure 8 Hilbert-Huang transform for RC1 (damage pattern 2): Sensor on the right side of the first floor.

In Figure 12, we showed the acceleration records of the first and second floors for damage pattern 4. To these signals, we applied a bandpass filter (bandpass(X,[37.5 48], Fs)) (it obtained from the Fourier transform). Then we used the EMD method; we presented the first intrinsic modal functions (IMF) for each of the floors in Figure 13. On all floors, there is a significant change in the behavior of the signal at the 40s. Additionally, we applied the Hilbert transform shown in Figure 14, where the frequency change is small since this damage pattern is medium damage. However, there is a significant change in the amplitude level at the 40s. The accelerations of the other floors have the same behavior.

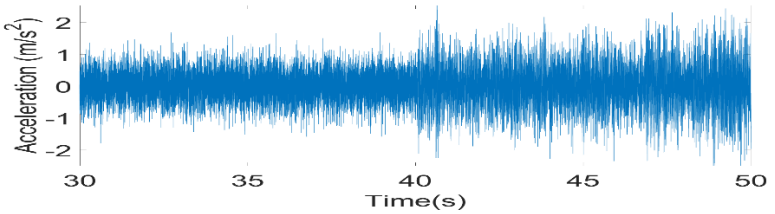

(a)

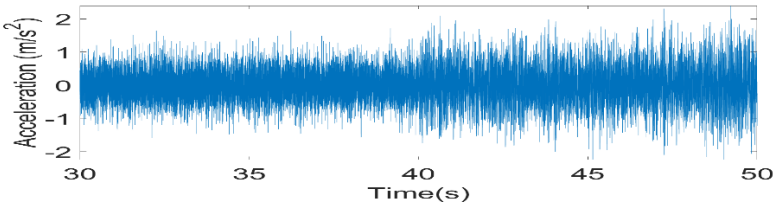

(b)

Figure 9 Acceleration records: (a) first floor, (b) second floor. All plots correspond to damage pattern 4 obtained from the sensor on the right side in the x direction.

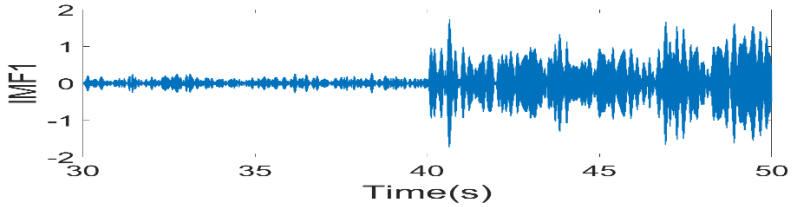

(a)

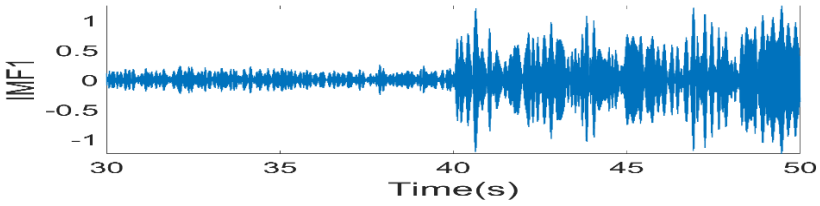

(b)

Figure 10 IMF 1: (a) first floor, (b) second floor. All plots correspond to damage pattern 4, obtained from the sensor on the right side in x direction.

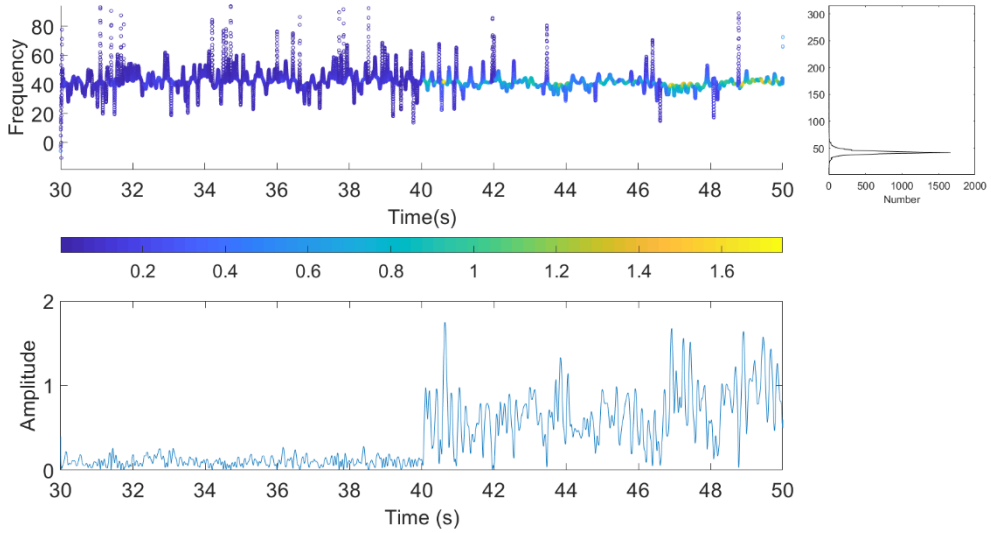

(a)

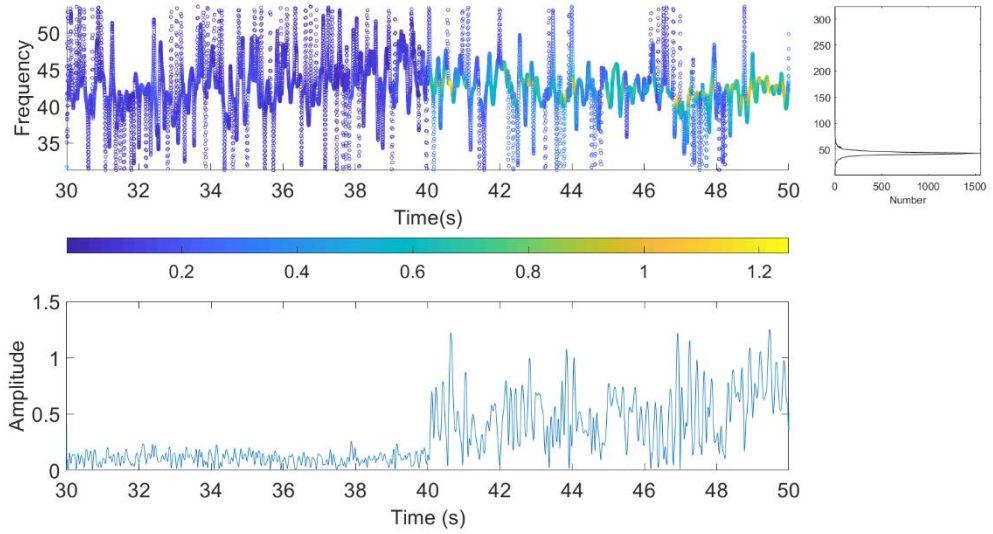

(b)

Figure 11 Hilbert-Huang transform for the first modal response: (a) first floor, (b) second floor. All plots correspond to damage pattern 4.

Then we applied the SSA. In Figure 15, we presented the reconstructed components (RC), where, unlike the EMD, it is not necessary to apply any filter. Although in the RC1 and RC2 components, we observed a change in the signal behavior at the 40s, we then applied the Hilbert transform to each of these RCs. In Figure 16, we presented the Hilbert transforms of RC1 for both sensors. Like the EMD, the frequency change is small, but it is clear that there is a significant change in the amplitude level at the 40s.

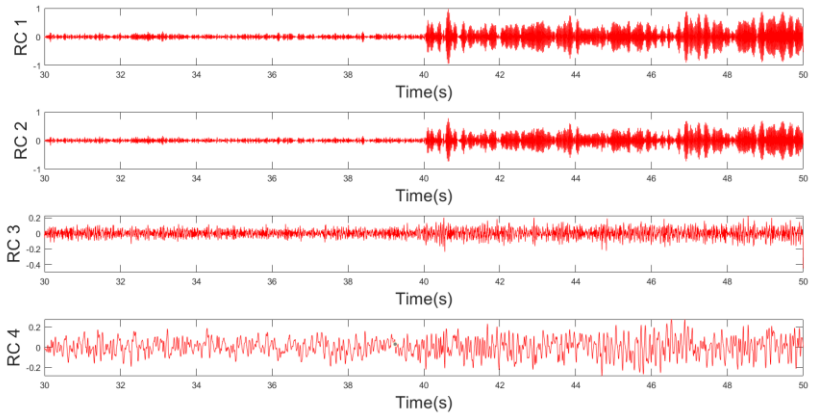

(a)

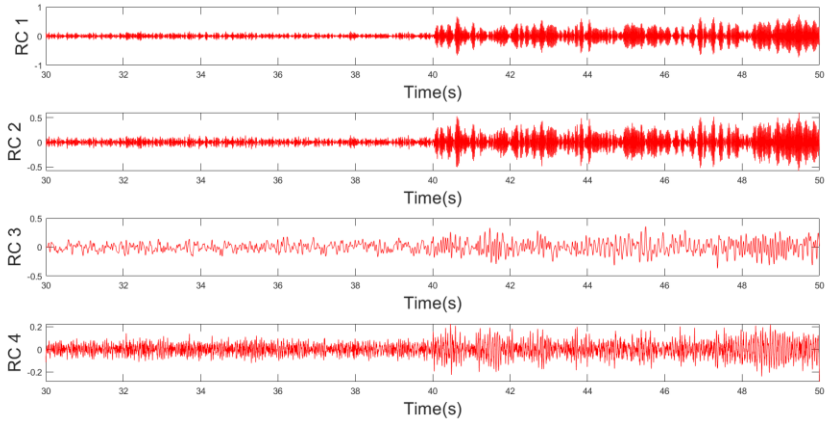

(b)

Figure 12 RC for damage pattern 4: (a) first floor, (b) second floor

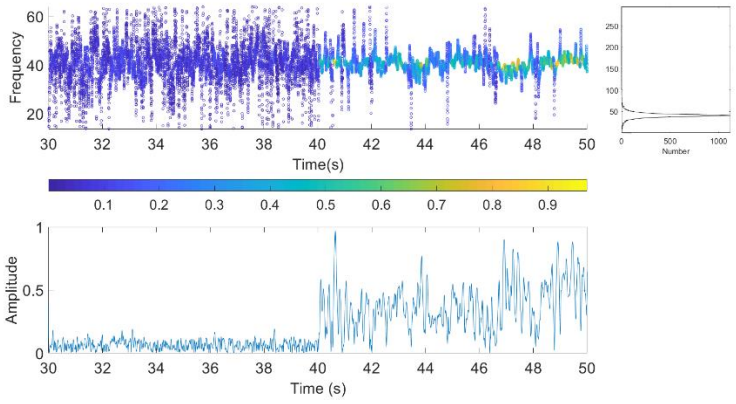

(a)

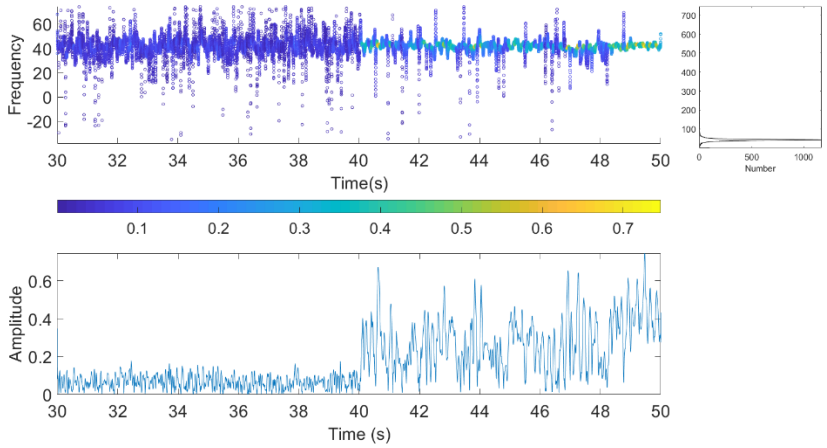

(b)

Figure 13 Hilbert-Huang transform for RC1 (damage pattern 4): (a) first floor, (b) second floor, (c) third floor, (d) fourth floor.

In Figure 17, we illustrated the acceleration record of of the first and second floors for damage pattern 6. To these signals, we applied a bandpass filter (bandpass (X,[37.5 48], Fs)) (it obtained from the Fourier transform). Subsequently, we used the EMD method; we presented the first IMF for each of the floors in Figure 18, where we observed that the signal changes at the 40s in floors 1 and 4. This is further verified when we applied the Hilbert transform (see Figure 19), where the frequency change is not so evident in any of the floors. However, on floors 1 and 4, we observed a change in the signal's amplitude at the 40s. In contrast, on floors 2 and 3, there is no significant change for this reason it was not necessary to include the graphs. This could indicate that the damage only occurs on floors 1 and 4.

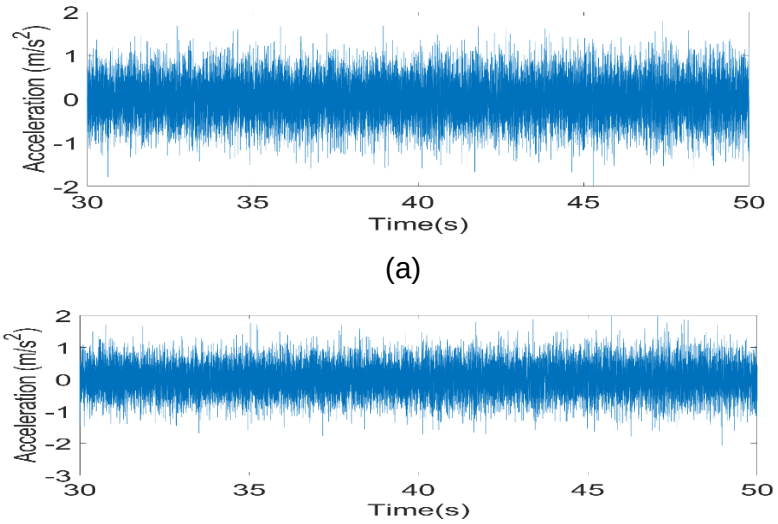

(a)

(b)

Figure 14 Acceleration records: (a) first floor, (b) fourth floor. All graphs correspond to damage pattern 6.

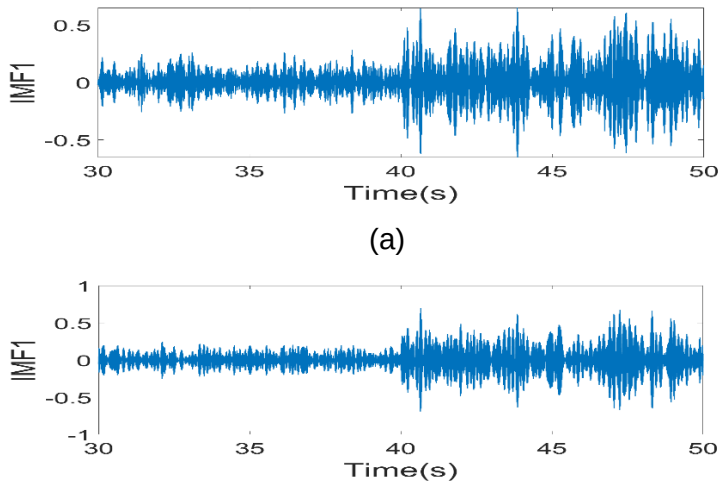

Figure 15. IMF 1: (a) first floor, (b) fourth floor. All graphs correspond to damage pattern 6.

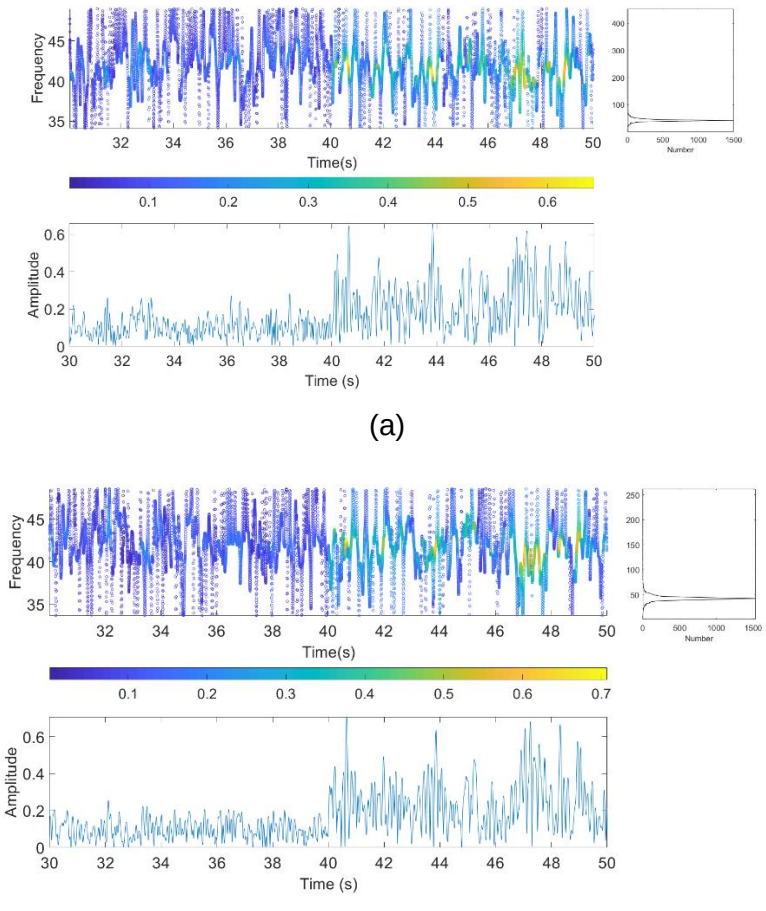

Figure 16 Hilbert-Huang transform for the first modal response: (a) first floor, (b) fourth floor. All plots correspond to damage pattern 6.

Then we applied the SSA; in Figure 20, we presented the reconstructed components (RC). Unlike the EMD, it is not necessary to apply any filter. On floors 1 and 4, we observe a change in the amplitude of the signal at the 40s, while in floors 2 and 3, there is no significant change; this could indicate that the damage only occurs in floors 1 and 4 or that the damage in floors 2 and 3 is too slight and the method does not detect it, we can verify this result in the amplitude levels shown in the Hilbert transform in Figure 21.

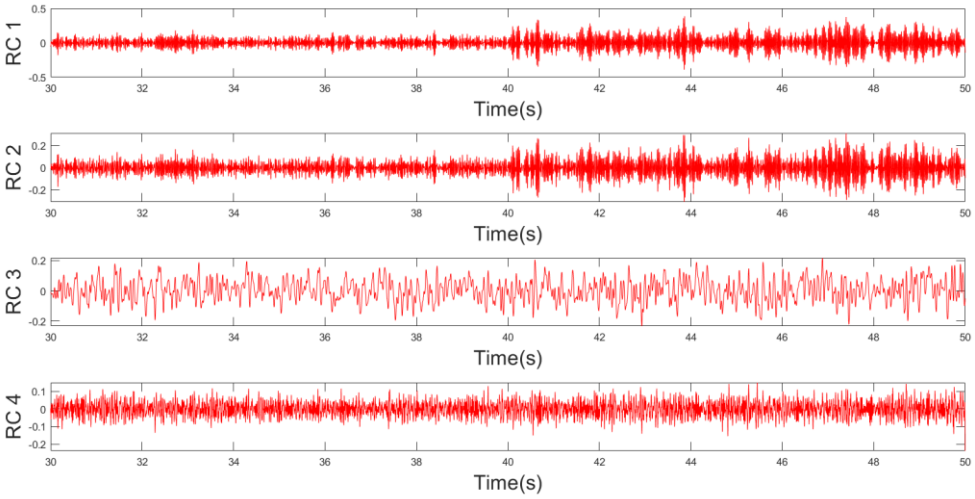

(a)

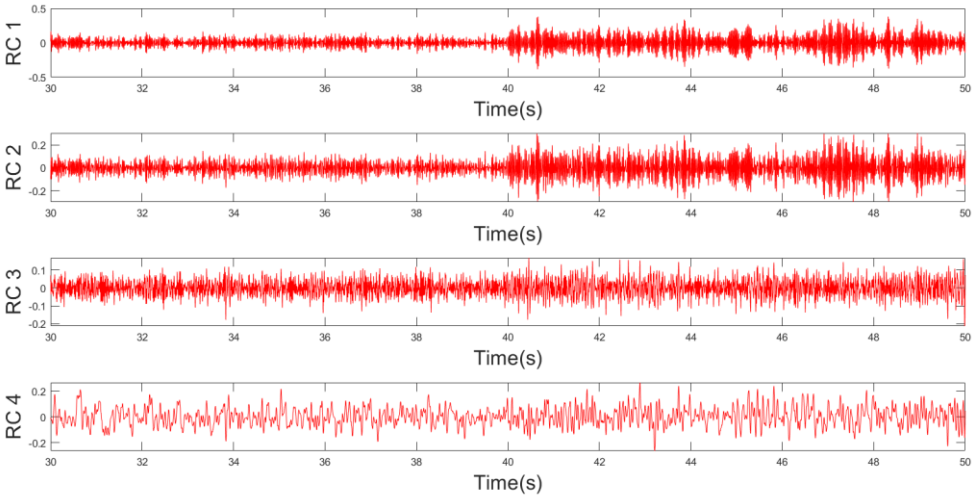

(b)

Fig 17. RC for damage pattern 6: (a) first floor, (b) fourth floor

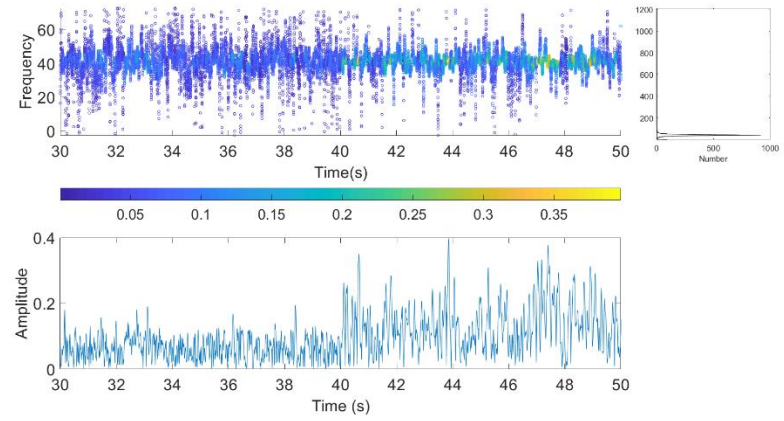

(a)

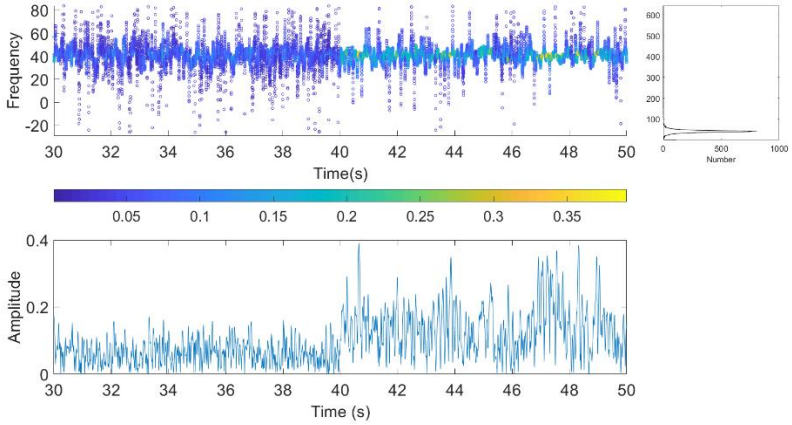

(b)

Figure 18 Hilbert-Huang transform for RC1 (damage pattern 6): (a) first floor, (b) fourth floor.

4.2 Comparative Analysis Between EMD and SSA

From the previous section, we could state that when the damage is severe, the characteristic frequency of the signal changes over time, so that the empirical distribution of the frequencies is bimodal, which indicates the presence of two characteristic frequencies of the signal, one before and the other after the damage. On the other hand, when there is no damage, the signal retains its fundamental frequency over time.

In order to evaluate the effectiveness of both methods, we proposed to perform a Monte Carlo type simulation study, in which initially we generated a vibration signal for each type of damage, like those performed in the previous section, where the noise is Normal of zero mean and one variance. The null hypothesis is that the distribution of frequencies is unimodal, in which case there is no change in the fundamental frequency of the signal, versus the alternative hypothesis of the presence of more than one mode, indicating structural damage. If the p-value of the statistical test is less than 0.05 (the significance

level), we reject the null hypothesis, and the test detects damage. To control the included random noise and other factors inherent to the simulation, we repeated the procedure 1000 times. The result of the 1000 simulations is the percentage of detection under each damage scenario.

In Figure 22, we showed the results of this simulation study, where we presented the detection percentage for each of the methods. We concluded that for severe damage, both methods identify the damage ideally. However, for damage patterns 3, 4, and 6, the detection capacity of both methods, evaluated through the identification of the change in frequencies, decreases substantially. This result is because, for these damage patterns, the frequency variation is 1 Hz or less, as presented in [18]. Generally, SSA presents better statistics than EMD. The script to apply the hypothesis test was done in Python language.

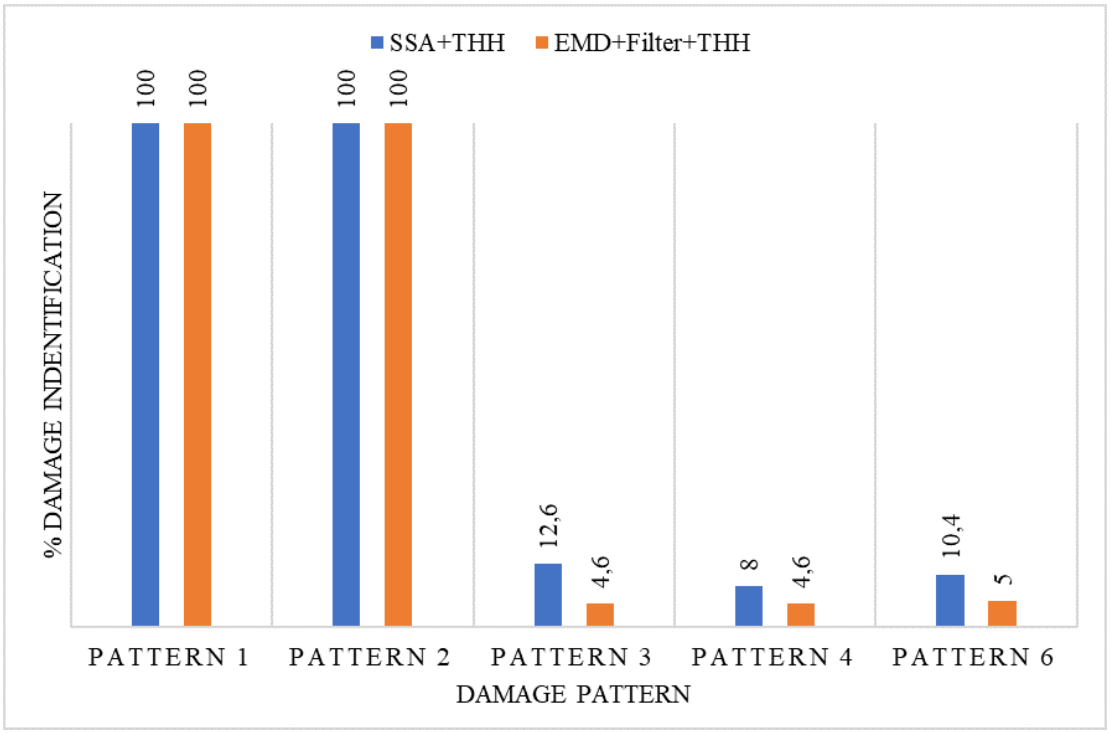

Figure 19 Percentage of damage identification for each method

5. Conclusions

The EMD method, along with a high pass filter, detects severe damage when the acceleration records have low or no noise.

When the acceleration records are contaminated with noise, the likelihood of the EMD detecting the damage decreases dramatically. To reduce the noise phenomenon, we used the Hilbert transform. Then, the EMD, along with a bandpass filter and Hilbert transform, allows the detection of severe, medium, and light damage with a noise level of 10%.

The SSA method and highpass filters detect severe damage when the acceleration records have low or no noise.

When the acceleration records are contaminated with noise and the damage patterns are severe (patterns 1 and 2), the SSA, a bandpass filter, and Hilbert transform can effectively detect the damage.

When the damage is medium or mild (patterns 3, 4, and 6), the SSA detects the damage without any filter and it is not necessary to apply the Hilbert transform in any of its components (RC).

One of the advantages of the SSA over the EMD is that, for medium or mild damage patterns, the SSA does not require filters or the use of the Hilbert transform to detect the damage.

When the damage is severe, both methods showed a noticeable change in the fundamental frequency. However, when the damage is slight, the change in fundamental frequency is not apparent. But we observed a significant change in the amplitude level. In general, we found that SSA is more effective in detecting damage.

References

[1] C.-H. Loh, C.-H. Chen and T.-Y. Hsu, "Application of advanced statistical methods for extracting long-term trends in static monitoring data from an arch dam," Structural Health Monitoring, vol. 10, pp. 587-601, Noviembre 2011. https://doi.org/10.1177/1475921710395807

[2] L. Chin-Hsiung, C. Chia-Hui and M. Chien-Hong, "Detecting seismic response signals using singular spectrum analysis," Sensors and Smart Structures Technologies for Civil, Mechanical, and Aerospace Systems 2010, vol. 7647, pp. 535 -546, 2010. https://doi.org/10.1117/12.846427

[3] Medina, B. y Duque, L. “Fuzzy entropy relevance analysis in DWT and EMD for BCI motor imagery applications”. Ingeniería, Vol. 20, No. 1, pp. 9–19, 2015. https://doi.org/10.14483/udistrital.jour.reving.2015.1.a01

[4] E. Johnson, H. Lam, L. Katafygiotis and J. Beck, "Phase I IASC-ASCE Structural Health Monitoring Benchmark Problem Using Simulated Data," Journal of Engineering Mechanics, vol. 130, no. 1, pp. 3-15, 2004. https://doi.org/10.1061/(asce)0733-9399(2004)130:1(3)

[5] G. Gilbert-Rainer and P. Zeno-Iosif, "Modal identification and damage detection in beam-like structures using the power spectrum and time–frequency analysis," Signal Processing, pp. 29-44, 2014. https://doi.org/10.1016/j.sigpro.2013.04.027

[6] D. Pines and L. Salvino, "Structural health monitoring using empirical mode decomposition and the Hilbert phase," Journal of Sound and Vibration, vol. 294, no. 1, pp. 97-124, 2006. https://doi.org/10.1016/j.jsv.2005.10.024

[7] N. Cheraghi and F. Taheri, "A damage index for structural health monitoring based on

the empirical mode decomposition," Journal of Mechanics of Materials and Structures - J MECH MATER STRUCT, vol. 2, pp. 43-61, Marzo 2007. https://doi.org/10.2140/jomms.2007.2.43

[8] L. Cano, "On Time-Frequency Analysis for Structural Damage Detection," PhD. Thesis, University of Puerto Rico, Puerto Rico, 2008. Available: https://www.researchgate.net/publication/257138876_On_Time-Frequency_Analysis_for_Structural_Damage_Detection

[9] D. Swagato and S. Purnachandra, "Structural health monitoring techniques implemented on IASC-ASCE benchmark problem: a review," Journal of Civil Structural Health Monitoring, 2018. https://doi.org/10.1007/s13349-018-0292-5

[10] B. Basuraj , H. Budhaditya and P. Vikram, "Real time structural damage detection using recursive singular spectrum analysis," 13th International Conference on Applications of Statistics and Probability in Civil Engineering, ICASP13, pp. 1-8, 2019. Available: https://s-space.snu.ac.kr/bitstream/10371/153487/1/358.pdf

[11] S. Sony and A. Sadhu, "Multivariate emplirical mode decomposition-based structural damage localization using limited sensors," Journal of Vibration and Control, vol. 0, no. 0, pp. 1-13, 2021. https://doi.org/10.1177/10775463211006965

[12] D. Yansong, S. Zongzhen and G. Kongzheng, "Structural damage identification under variable environmental/operational conditions based on singular spectrum analysis and statistical control chart," Structural Control and Health Monitoring, vol. 28, no. 6, pp. 1-19, 02 March 2021. https://doi.org/10.1002/stc.2721

[13] J. I. Campos Hernández, "Innovador método para detectar daño estructural, funciones de la bifurcación frecuencial modal (modal frequency splitting functions)," DSpace Home, 2018.

[14] R. Zhang, M. Asce, S. Ma, E. Safak and S. Hartzell, "Hilbert-Huang Transform Analysis of Dynamic and Earthquake Motion Recordings," Journal of Engineering Mechanics-asce - J ENG MECH-ASCE, vol. 129, 2003. https://doi.org/10.1061/(asce)0733-9399(2003)129:8(861)

[15] L. Plazas, M.A. Avila, A. Torres, “Spectral Estimation of UV-Vis Absorbance Time Series for Water Quality Monitoring” Ingeniería, vol. 22, no. 2, pp. 211-225, 2017. https://doi.org/10.14483/udistrital.jour.reving.2017.1.a01

[16] K. Liu, S. Law, Y. Xia and X. Zhu, "Singular spectrum analysis for enhancing the sensitivity in structural damage detection," Journal of Sound and Vibration, vol. 333, no. 2, pp. 392-417, 2014. https://doi.org/10.1016/j.jsv.2013.09.027

[17] M. A. de Oliveira, J. V. Filho, V. Lopes and D. J. Inman, "A new approach for structural damage detection exploring the singular spectrum analysis," Journal of Intelligent Material Systems and Structures, vol. 28, no. 9, pp. 1160-1174, 2017. https://doi.org/10.1177/1045389x16667549

[18] J. Yang, Y. Lei, S. Lin and N. Huang, "Hilbert-Huang Based Approach for Structural Damage Detection," Journal of Engineering Mechanics, vol. 130, no. 1, pp. 85-95, 2004. https://doi.org/10.1061/(asce)0733-9399(2004)130:1(85)